Fine-grained Appearance Transfer with Diffusion Models

YuTeng Ye[1], Guanwen Li[1], Hang Zhou[1], Jiale Cai[1], Junqing Yu[1],
Yawei Luo[2], Zikai Song[1], Qilong Xing[1], Youjia Zhang[1], Wei Yang[1]
[1]Huazhong University of Science & Technology,
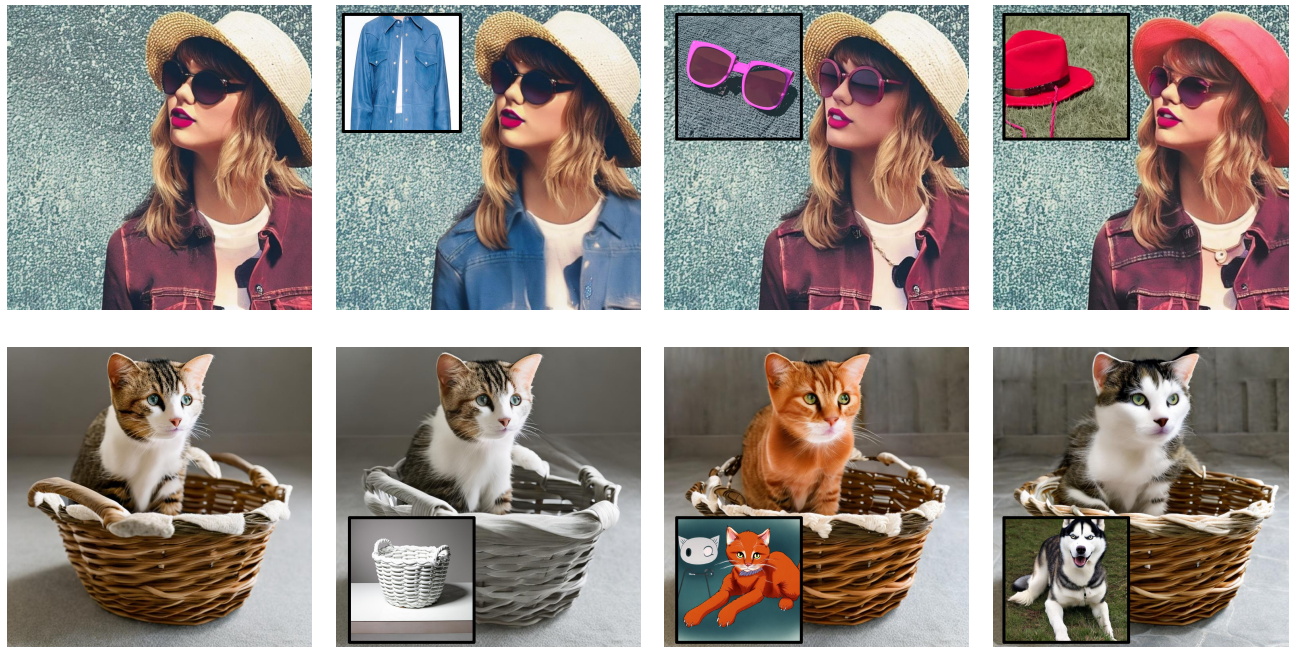[2]Zhejiang University

Figure 1. The results of fine-grained appearance transfer using our method. The leftmost column displays the source images. On the right, the output images achieved by detailed appearance transfer corresponding to the target images (outlined in black), while preserving structural integrity. The examples at the bottom demonstrate our method's capability to transfer across various domains and categories.

Abstract

Image-to-image translation (I2I), and particularly its subfield of appearance transfer, which seeks to alter the visual appearance between images while maintaining structural coherence, presents formidable challenges. Despite significant advancements brought by diffusion models, achieving fine-grained transfer remains complex, particularly in terms of retaining detailed structural elements and ensuring information fidelity. This paper proposes an innovative framework designed to surmount these challenges by integrating various aspects of semantic matching, appearance transfer, and latent deviation. A pivotal aspect of our approach is the strategic use of the predicted x_0 space by diffusion models within the latent space of diffusion processes. This is identified as a crucial element for the precise and natural transfer of fine-grained details. Our framework exploits this space to accomplish semantic alignment between source and target images, facilitating mask-wise appearance transfer for improved feature acquisition. A significant advancement of our method is the seamless integration of these features into the latent space, enabling more nuanced latent deviations without necessitating extensive model retraining or fine-tuning. The effectiveness of our approach is demonstrated through extensive experiments, which showcase its ability to adeptly handle fine-grained appearance transfers across a wide range of categories and domains. We provide our code at https://github.com/babahui/Fine-grained-Appearance-Transfer

arXiv:2311.16513v1 [cs.CV] 27 Nov 2023

1. Introduction

Image-to-image translation (I2I) stands as a cornerstone task in computer vision, which primarily focuses on transforming images from a source domain to a corresponding target domain. Within the I2I spectrum, a notable sub-task is appearance transfer. The primary objective here is to transpose the visual aesthetics of a target image onto a source image, concurrently preserving the structural essence of the source image. Nonetheless, this task often grapples with complexities in achieving fine-grained transfer, especially in retaining intricate structures and upholding information fidelity.

The advent of diffusion models has catalyzed remarkable progress in the field, propelled by the emergence of large-scale models [28–30] and expansive datasets [31, 32]. These models have risen to prominence due to their efficacy in various image translation tasks. However, their application in fine-grained appearance transfer encounters significant hurdles, primarily in two areas:

- **Representation of Fine-Grained Information:** While current methods [3, 11, 16] often rely on text-based guidance for image generation within diffusion models, achieving precision in fine-grained control remains an elusive goal. This is attributed to the inherent challenges in pinpointing specific details and processing nuanced information. Conversely, image-guided methods offer a more direct approach by leveraging the abundant structural and semantic details intrinsic to images. However, some strategies, such as encoding the target image into low-level features for guiding generation [36, 38], can inadvertently oversimplify the visual appearance, thus losing critical fine-grained details.
- **Fine-Grained Appearance Transfer:** Methods employing contrastive learning based on structural and appearance similarities [18, 36] often face the challenge of losing semantic and structural nuances during the transfer process. Recent developments in diffusion features [35] have demonstrated potent capabilities in establishing precise point-to-point correspondence, aiding in meticulous matching and transfer. SD-DINO [40], for instance, uses pixel-level swapping based on these correspondences for an initial coarse transfer, but requires additional refinement and lacks adaptability across diverse domains and categories.

In response to these challenges, we propose a novel framework integrating Semantic Matching, Appearance Transfer, and Latent Deviation components. Our innovative approach hinges on the exploitation of the x_0 space, an integral data-informed component extracted from the latent space of diffusion models, identified as key to facilitating natural and precise fine-grained information transfer. Specifically, our method involves establishing a semantic alignment between source and target images within the x_0 space, leveraging the robust semantic relationships inherent in diffusion features. This alignment enables mask-wise appearance transfer to attain the desired feature. The transferred feature is then smoothly integrated into the latent space, undergoing a linear refinement of the intermediate latent representation and the generation of adaptive noise. This novel approach ensures a seamless transition from the x_0 space to the latent space, negating the necessity for extensive model training or fine-tuning. Through the aforementioned process, we devise a modified latent trajectory that gradually transitions towards the target domain.

Our contributions are delineated as follows:

- We identify the x_0 space as optimal for appearance transfers and implement semantic matching to capture fine-grained details effectively.
- We engineer a fluid transition from the x_0 space to the latent space, obviating the need for model retraining or extensive fine-tuning.
- Our empirical evaluations validate the efficacy of fine-grained appearance transfers across diverse categories and domains, underscoring the method's versatility and robustness.

2. Related Work

Our work aims at fine-grained appearance transfer, representing a challenging sub-problem in the realm of Image-to-Image Translation.

2.1. Image-to-Image Translation

Image-to-Image Translation (I2I) involves transforming images from a source domain to a target domain. Previous research [5, 8, 14, 15, 19, 37, 39] primarily focused on models based on GANs [9], yet adapting these models to diverse image domains has been challenging [34]. The advent of diffusion models [28, 29] has brought significant advancements, offering enhanced flexibility and broader applicability in various contexts [4, 17]. A specific subset of I2I is fine-grained appearance transfer. This subdomain concentrates on transferring visual appearance with an emphasis on preserving structural details and fidelity. While several studies [4, 20] have addressed fine-grained transfer, consistently achieving high-quality results in a wide range of scenarios remains a substantial challenge. Our work is dedicated to this aspect, seeking to adapt fine-grained appearance transfer for broad applicability across diverse categories and domains.

2.2. Predicted x_0 Feature in Diffusion Model

In the denoising process of diffusion models, noisy latent features are projected to an estimated x_0 feature, which encapsulates clean information. Several research methodolo-

gies have been developed based on this feature. For example, SAG [13] utilizes Gaussian blur to reduce redundant information in x_0 feature, thereby enhancing sample quality. Additionally, General I2I [4] focuses on minimizing the distance between x_0 features to reconstruct the original image. Other methods [18] employ an image encoder to process the x_0 feature and then transfer it with structural or appearance constraints. In contrast to these approaches, our primary goal is to facilitate the transfer of fine-grained information at the x_0 feature level. Our approach differs from methods like those in [18] that encode the x_0 feature through a model; instead, we engage in fine-grained semantic matching directly within the x_0 feature. This approach ensures the preservation of detailed structural integrity and information fidelity.

2.3. Feature Correspondence

Feature correspondence in generative models establishes dense connections among features derived from a range of visual appearances and categories. Initially, methods like SIFT [7] and HOG [6] relied on hand-designed features. The introduction of deep generative models such as GANs [10] represented a shift from these traditional approaches, contributing to the identification of visual correspondences in diverse image domains [24, 26, 41]. Recent advances, exemplified by DIFT [35], have shown that diffusion models' intermediate features exhibit robust point-to-point correspondence. Utilizing this feature, various studies have applied feature correspondence to downstream tasks. DIFT [35] uses these correspondences for affine transformations from a target to a source image. DragonDiffusion [22] applies a feature correspondence loss to guide the editing of intermediate features. Additionally, SD-DINO [40] combines elements from DINO [2] and Stable Diffusion to compute feature correspondences for object swapping. Contrasting with SD-DINO [40], which focuses on swapping within the same categories, our work extends to a broader range of appearance transfer scenarios, including transfers across different domains and categories.

3. Methods

3.1. Preliminaries

Similar to DDPM [12], DDIM [33] reconstructs an image from white noise through an iterative denoising process. DDIM, aiming to accelerate the sampling process of DDPM while ensuring the quality of generated images, devises a process with fewer steps and a non-Markovian nature. Formally, given an image x_0 and a variance schedule β_t at timestep t, the generation process in DDIM is deterministic. The latent x_t comprises the predicted x_0 and a component directed towards x_t, which can be described by the following equation:

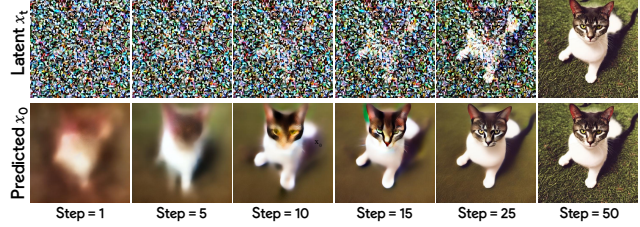Figure 2. Illustration of DDIM Sampling Steps with Latent Feature x_t and Predicted x_0. Here, we apply a latent decoder to convert both predicted x_0 and x_t into the image for visualization.

$$x_{t-1} = \sqrt{\alpha_{t-1}} \underbrace{\left(\frac{x_t - \sqrt{\beta_t}\epsilon_\theta^{(t)}(x_t)}{\sqrt{\alpha_t}} \right)}_{\text{" predicted } x_0\text{"}} + \underbrace{\sqrt{\beta_{t-1}} \cdot \epsilon_\theta^{(t)}(x_t)}_{\text{"direction pointing to } x_t\text{"}}$$

(1)

where $\alpha_t = 1 - \beta_t$, and $\epsilon_\theta^{(t)}$ denotes a neural network parameterized by $\theta^{(t)}$. In Eq. (1), the latent variable representation x_t can be viewed as a blend of the data-informed component $x_0^{(t)}$ and the noise-driven term $\epsilon(x_t)$, formalized as:

$$x_t = \sqrt{a_t}x_0^{(t)} + \sqrt{1 - a_t}\epsilon_\theta^{(t)}(x_t)$$

(2)

For brevity in subsequent sections, we denote the term $\epsilon_\theta^{(t)}(x_t)$ as $\epsilon(x_t)$, and $x_0^{(t)}$ as x_0.

3.2. Problem Formulation

Our proposed framework aims to facilitate a detailed, fine-grained synthesis between a source image I and a target image T. This process entails the precise transfer of visual appearance from I to T, with an emphasis on maintaining the structural integrity of I. The primary challenges in this fine-grained transformation include:

- **Detail Alignment**: Achieving accurate alignment of fine-grained details between I and T, crucial for preserving the structural integrity of objects during the transformation process.
- **Fine-grained Appearance Transformation**: Implementing a transformation that meticulously aligns with semantic and structural nuances across different domains and categories, thus enabling a seamless and coherent integration of visual elements.

3.3. Overall Framework

As depicted in Fig. 3, our methodology initiates by applying null-text inversion [21] to the source image I along with the associated source prompt, optimizing unconditional text embedding at each step to create a latent path $\{x_t, x_{t-1}, \ldots, x_0\}$ for reconstructing I. Concurrently,
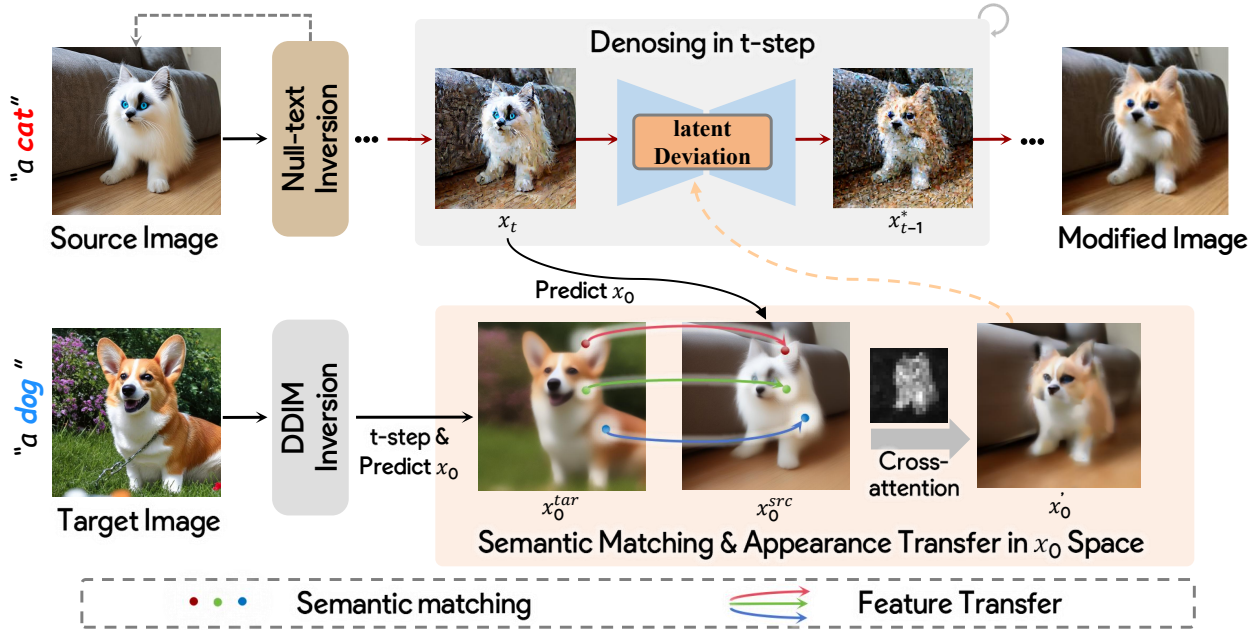
Figure 3. **Our Pipeline.** This figure illustrates our pipeline, commencing with null-text inversion applied to the source image I, creating a latent path for reconstructing the image. During the diffusion denoising stage, Latent Deviation is performed, leading to a modified image that aligns with the target image T. Specifically, the process begins with semantic alignment in the x_0 space between x_0^{src} and x_0^{tar}, where x_0^{tar} is obtained through DDIM inversion with T. Based on semantic relations, features from x_0^{tar} are transferred to x_0^{src}, guided by an attention mask of I, resulting in x_0'. Finally, x_0' is processed in the latent space to synthesize the final modified image.

DDIM inversion [33] is applied to the target image T and its corresponding target prompt, progressively introducing noise to transition into the latent space. Throughout this process, we predict the t-step x_0^{tar} image feature from its latent code using Eq. (2).

The framework integrates two pivotal concepts: Semantic Matching & Appearance Transfer and Latent Deviation. These approaches allow us to alter the generation path of x_t using x_0^{tar}, a strategy informed by our insights into the x_0 space. We observe a notable potential for manipulating image features in this space while maintaining structural integrity.

Observations in x_0 Space. Our analysis, as shown in Fig. 2, uncovers a key finding: the initial latent code x_0 exhibits a higher fidelity in capturing fine-scale details compared to the noisier x_t. Particularly in the early stages of the diffusion process, x_0 plays a crucial role in reconstructing the object's structure, progressively evolving to encapsulate more complex details. We define the series of steps involving x_0 as the x_0 space, which emerges as a vital medium for information transfer between images. Transferring features in the x_0 space effectively minimizes perturbations induced by latent noise, thereby preserving and conveying high-fidelity details during image synthesis.

Semantic Matching and Appearance Transfer. Our objective is to achieve a semantic-aligned visual appearance transfer from a source image to a target image. We propose utilizing the x_0 space for this transformation due to its capability to retain structured and fine-scale image features. To facilitate this transfer within the x_0 space, establishing a semantic alignment between the source and target is crucial. We employ the DIFT Feature [35], which demonstrates strong relations across different domains and categories, for semantic matching in the x_0 space. Specifically, given a source image feature x_0^{src} and a target image feature x_0^{tar} at step t, we input them into a diffusion model to extract their respective DIFT features. We then compute the point-to-point cosine distance between these features, ranking these distances to form a correlation mapping $\mathcal{C}$ from source to target. Lastly, we perform a mask-wise transfer in the x_0 space, targeting only the primary objects for transformation while preserving the background. This whole transfer approach in x_0 space is formulated as:

$$x_0' = \mathcal{M}\left((1-\delta)x_0^{\text{src}} + \delta\mathcal{C}(x_0^{\text{tar}})\right) + (1-\mathcal{M})x_0^{\text{src}} \quad (3)$$

where x_0' represents the transferred image feature, $\mathcal{M}$ denotes a cross attention mask applied to primary objects in source image. δ signifies the weight of the transfer, and $\mathcal{C}(x_0^{\text{tar}})$ represents the features of x_0^{tar} that are matched in x_0^{src}. We simplify the appearance transfer described in Eq. (3) as follows:

$$x_0' = x_0 + \mathcal{T}(x_0', x_0) \quad (4)$$
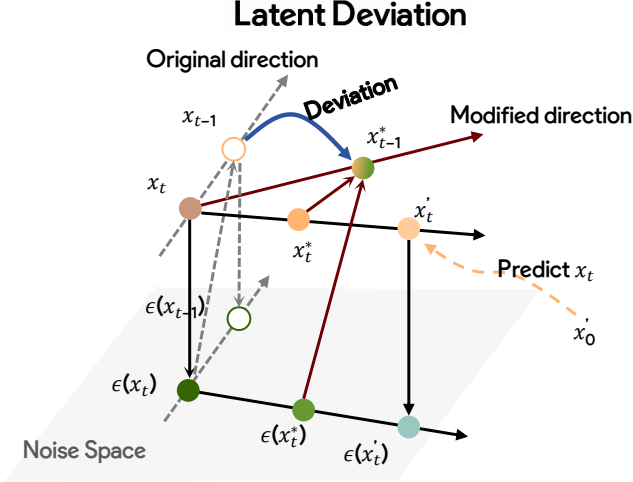
Latent Deviation

Figure 4. **Latent Deviation Process.** Dashed lines represent the original latent path for image reconstruction, while solid red lines indicate the modified latent trajectory. Initially, the transferred x'_0 from Fig. 3 is transformed into its corresponding latent code x'_t and its noise component $\epsilon(x'_t)$. Subsequently, a linear update refines the intermediate latent representation x^*_t and adjusts the noise term $\epsilon(x^*_t)$. Finally, x^*_t and $\epsilon(x^*_t)$ undergo a forward DDIM pass, leading to the next denoising step and producing x^*_{t-1}. This step highlights the deviation from the original x_{t-1} to the modified x^*_{t-1} at step t.

Here, $\mathcal{T}(x'_0, x_0)$ denotes the transformation from x_0 to x'_0.

Latent Deviation. The next stage, termed "Latent Deviation," involves transitioning the transferred x'_0 into a latent space for smoother processing, as depicted in Fig. 4. The transition begins by converting x'_0 to a latent code x'_t according to Eqs. (2) and (4), which is expressed by the following equation:

$$x'_t = \sqrt{a_t}(x_0 + \mathcal{T}(x'_0, x_0)) + \sqrt{1 - a_t}\epsilon(x_t) \quad (5)$$

Here, we propagate appearance differences, represented by $\mathcal{T}(x'_0, x_0)$, to x'_t. Following this, x'_t is processed through a U-Net to derive its noise component $\epsilon(x'_t)$, indicating the current noise direction toward x'_t. Instead of directly using x'_t for further processing, we compute a smoother latent representation, given by:

$$x^*_t = \lambda x_t + (1 - \lambda)x'_t \quad (6)$$

where λ represents the balance coefficient. The noise term $\epsilon(x^*_t)$ is then updated as a linear mixture:

$$\epsilon(x^*_t) = \gamma\epsilon(x_t) + (1 - \gamma)\epsilon(x'_t) \quad (7)$$

In the denoising process, x^*_t and $\epsilon(x^*_t)$, which are aligned with the target domain, are input into a subsequent forward pass through the DDIM. This results in obtaining x^*_{t-1} for the next denoising step. The whole la-

tent deviation path in the denoising process is denoted as $\{x_t, x^*_{t-1}, x^*_{t-2}, \ldots, x^*_{t-k}\}$.

Framework Explanation. Our method smoothens the transfer of appearance differences from the x_0 space to latent deviations. To further analyze the denoising process from step t to $t-1$, we substitute Eqs. (5) to (7) into Eq. (1). This yields the following refined formulation:

$$
\begin{aligned}
x^*_{t-1} =& \sqrt{\alpha_{t-1}}(x_0 + (1 - \lambda)\mathcal{T}(x'_0, x_0)) \\
& + \sqrt{1 - a_{t-1}}\epsilon(x^*_t) \\
& + \sqrt{\frac{a_{t-1}(1 - a_t)}{a_t}}(\epsilon(x_t) - \epsilon(x^*_t))
\end{aligned} \quad (8)
$$

Here, $(1-\lambda)\mathcal{T}(x'_0, x_0)$ represents the shift within the x_0 space towards the target domain and the noise term $\epsilon(x^*_t)$ serves as a construct directing towards x^*_t. The term $\epsilon(x_t) - \epsilon(x^*_t)$ is tailored to adapt to the denoising process.

4. Experiment

Implementation details. We conduct experiments on a single NVIDIA V100 GPU using Stable Diffusion v2 [29]. In the initial phase, we apply null-text inversion to fine-tune unconditional text embedding. Our sampling process then proceeds without requiring any further model training or fine-tuning. For semantic matching, we employ DIFT matching [35] to obtain $\mathcal{C}$ in Eq. (3). We set the parameter δ in Eq. (3) to 0.6, regulating the extent of feature transfer. Additionally, we configure λ in Eq. (6) to 0.2, and γ in Eq. (7), which updates the unconditional noise component, is also set to 0.2. We set the start step to 12 to achieve a stable attention map. We set the end step at 21 based on observations of stable transfer achieved in the generated images.

Datasets. For evaluating our method, we collect data from both synthetic and real-world sources, as there is no standard dataset specifically tailored to our task. We generate synthetic data in a two-step process. First, we generate source and target text pairs using online ChatGPT-4 [25], covering a semantic range from closely related concepts (*e.g.* "dog" to "Welsh Corgi") to those with larger gaps (*e.g.* "dog" to "panda"), or from different domains (*e.g.* "a photo of a cat" to "an animation-style image of a cat"). We then process these text prompts through Stable Diffusion [29] to produce images. From this process, we manually select 400 pairs of high-quality source and target images for our evaluations, ensuring a diverse representation of scenarios including landscapes and animals. Additionally, we compile a set of 100 real-world images with related source and target text. These images are sourced and downloaded from the internet, adhering to permissible conditions.

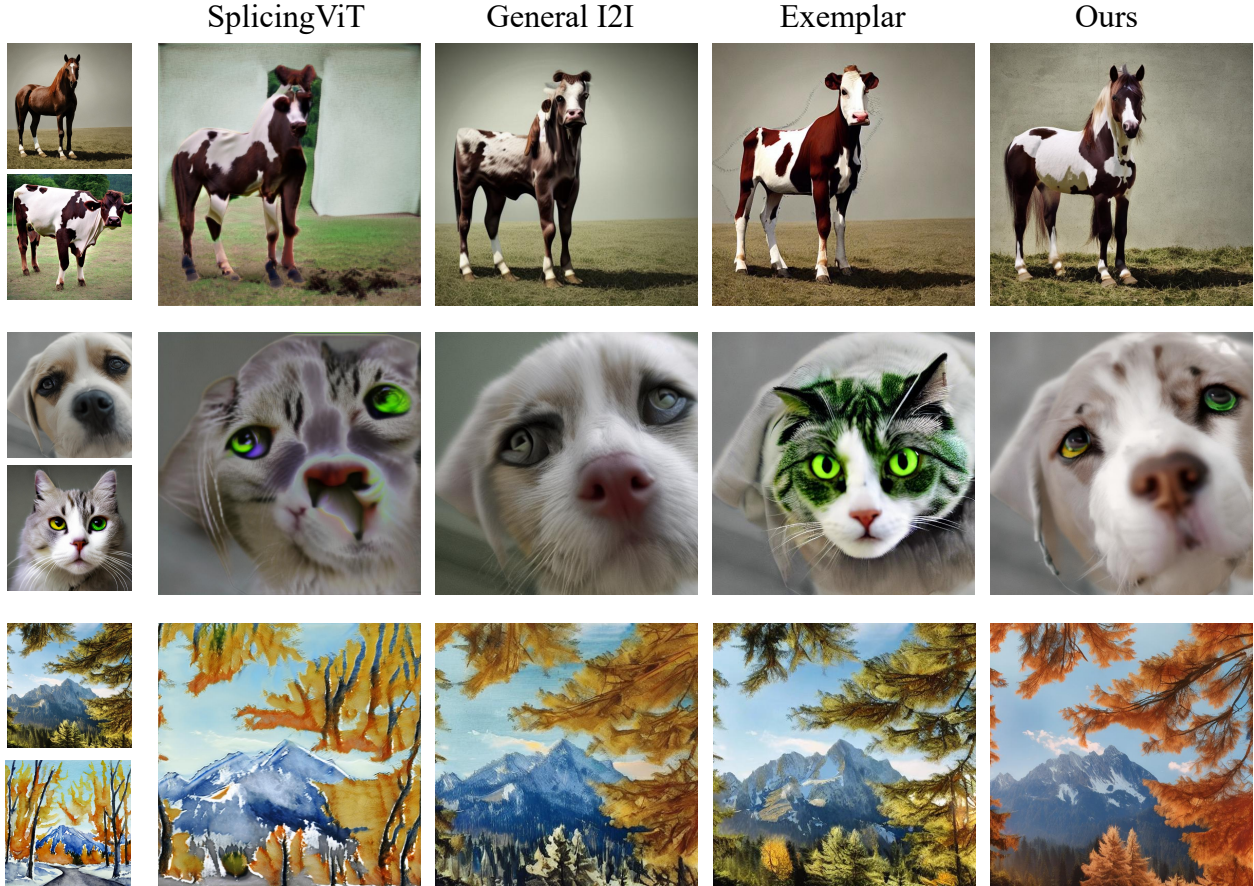| SplicingViT | General I2I | Exemplar | Ours |

Figure 5. **Qualitative Comparisons with Image-Guided Transfer Methods.** The figure showcases appearance transformations in three sets, arranged from top to bottom: from "horse" to "cow", "dog" to "cat" in a face swap, and from a real photo to a painting. In each set, the leftmost images are the source (top) and target (bottom).

Method	CLIPscore ↑	USERscore ↑	Total Cost Time
SplicingViT [36]	0.273	34.8	∼1h
General I2I [4]	0.289	64.5	∼30min
Exemplar [38]	0.268	31.7	-
Ours	**0.301**	**75.1**	∼3min

Table 1. **Quantitative comparison with Image-guided Transfer Methods.**

4.1. Comparison to Current Work

Qualitative and Quantitative Comparisons with Image-guided Transfer Methods. We compare our method with three current image-guided transfer approaches, including two diffusion models [4, 38] and one ViT-based method [36]. SplicingViT [36] primarily focuses on transferring semantic appearance, while General I2I [4] addresses a wide range of image-to-image translation tasks, translating visual concepts across different domains. Ex-

emplar [38] incorporates an attention mechanism [21] for generating necessary input masks. Additionally, we did not include SD-DINO [40] in our comparison as it specializes in transferring identical objects and lacks comprehensive code availability. The qualitative results are shown in Fig. 5. SplicingViT tends to produce images with poor generation quality. General I2I retains the overall structure but struggles to effectively transfer fine details of appearance. As illustrated in the second row of Fig. 5, crucial details like the target species' eye color are missed. Exemplar achieves image-level appearance transfer but lacks detail alignment, evident in the first row of Fig. 5 where the color region on the cow's back is inaccurately transferred, possibly due to the use of image encoding. Furthermore, these methods do not perfectly preserve detailed structure and information fidelity. For example, as shown in the first row of Fig. 5, the shape of the horse's ears is not accurately maintained, and in the second row, the eye color is not effectively transferred. Our result demonstrates the superiority of our method in achieving fine-grained appearance transfer.
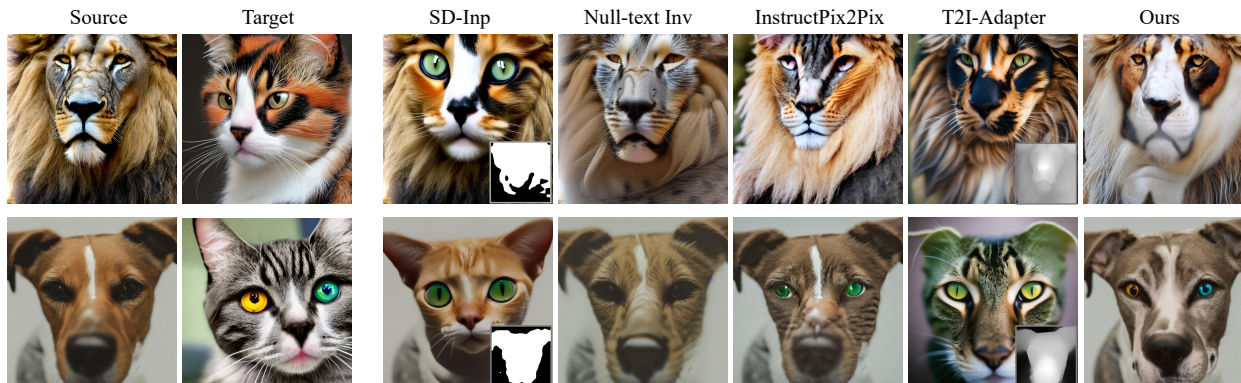
Figure 6. **Qualitative Comparisons with Text-Guided Transfer Methods.** For text input to text-guided methods, we generate detailed descriptions of target images using ChatGPT-4 [25].
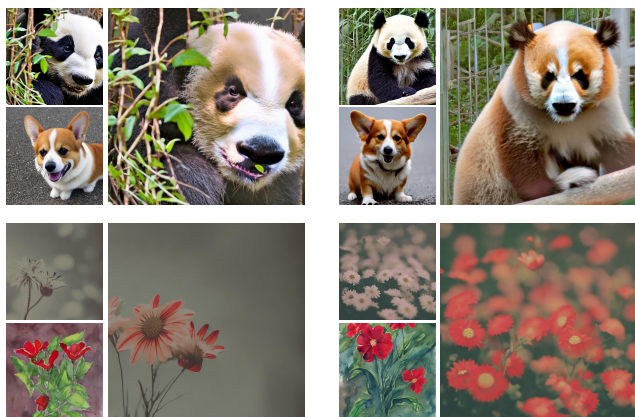

Figure 7. Results of our method in different domains and across large semantic gaps. The figure presents four sets of images: in each set, the top-left is the source image, the bottom-left is the target image, and the right side displays our output. The top two sets show the appearance transfer from "a panda" to "a dog", while the bottom two sets depict the transformation from realistic "flowers" to watercolor "flower".

We also conduct a quantitative evaluation with image-guided transfer methods. Due to the absence of ground truth for fine-grained appearance transfer, we assess the quality of appearance transfer from the following aspects: 1. To our knowledge, there is no dedicated metric specifically for measuring the quality of fine-grained transfer. Therefore, we conduct a user study where six human evaluators rate the transfer quality. Evaluators are asked to assess several aspects, including whether the overall appearance of the object is successfully transferred, whether the fine-grained transfer matches semantically, and whether the structural details are preserved. The user ratings range from 0 to 100, with higher scores indicating better quality of transfer. We calculate the average to determine the final score. 2. We utilize CLIP score [27] to evaluate the semantic sim-

ilarity between the source prompt and the output image, as our approach only involves appearance transfer, which is distinct from semantics. Quantitative results, as shown in Tab. 1, demonstrate that our method outperforms others in terms of CLIP score and user ratings. Regarding time efficiency, we compare the total sampling time, and our method is notably superior to others. The Exemplar method is not directly comparable because it requires approximately one week of model training in advance [38]. The primary time cost of our method is attributed to the initial Null-text inversion [21], with subsequent sampling processes requiring no additional model fine-tuning or training.

Qualitative Comparisons with Text-Guided Transfer Methods. We further evaluate the capability of fine-grained appearance transfer by comparing with text-guided image translation methods, including Stable Diffusion Inpainting (SD-inp) [29], T2I-Adapter [23], Null-text Inversion (Null-text Inv) [21], and InstructPix2Pix [1]. For these methods, we first obtain detailed text descriptions of the target image using online ChatGPT-4 [25], which are then input into the models to guide the image modification. The results are shown in Fig. 6. Our observations indicate that relying solely on text can be challenging for precisely controlling structural details and appearance. For example, as shown in the first row, using only text results in difficulties with accurately transferring specific facial structures, and in the second row, achieving exact eye color transfer through text alone is challenging.

To demonstrate the efficacy of our method across different domains and large semantic gaps, we present additional results in Fig. 7. As shown in the first row, our approach successfully transforms the appearance from "a panda" to "a dog," notably retaining the dog's color and texture in the process. This exemplifies our method's effectiveness in aligning semantically disparate elements in scenarios with large semantic gaps. The second row illustrates our capability to transfer appearances across different domains.

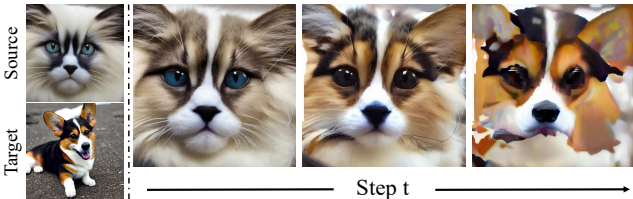Figure 8. Visualization of the Ablation Study on Method Components.

Figure 9. Visualization of the Ablation Study on End Step t. The figure shows the gradual evolution of our generated images as the end step t increases.

4.2. Ablation Study

Ablation Study on Method Components. We conduct an ablation study on each component of our method, including Semantic Matching (SM) and Latent Deviation (LD). As shown in Fig. 8, without SM, our method fails to accurately match appearances, leading to incorrect information transfer. Additionally, without LD, the transfer process becomes uneven, resulting in implausible outcomes. Overall, by employing all of our proposed components, we achieve the best generation outputs, which better preserve both structure and appearance.

Ablation Study of End Step t. End Step t represents the step in our diffusion sampling process where the transfer is concluded. As shown in Fig. 9, we find that the extent of appearance changes in our output images is closely correlated with the setting of the end step t. This correlation is due to the progressive transfer process we adopt. When t is set too low, the transfer may lack sufficient appearance features, leading to incomplete or ineffective transfer. Conversely, setting t too high can result in over-transfer, incorporating excessive or redundant appearance features from the target. This suggests that the optimal appearance transfer occurs at the mid-stage of diffusion denoising.

4.3. Limitation

Though achieving fine-grained appearance transfer, our method may fail under certain conditions, such as differing viewpoints and significant size discrepancies, as shown in Fig. 10. Due to differences in viewpoint, incorrect matches may occur between details in the source image (*e.g.* the front grille of the car) and the target image, leading to the transfer of inappropriate appearance information. Ad-
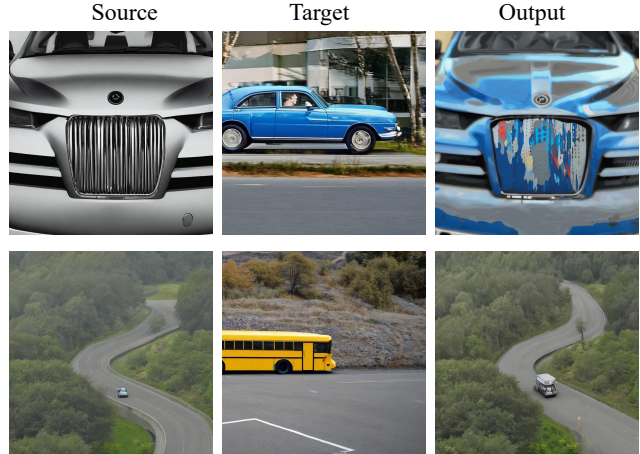

Figure 10. Illustration of failure cases of our method.

ditionally, if the main object in the source image is excessively small, the attention mask used in our method might be inaccurately positioned, resulting in erroneous appearance transfer.

5. Conclusion

In conclusion, this paper reports an important advancement in appearance transfer. We introduce a novel framework that effectively overcomes challenges in fine-grained transfer, utilizing the distinctive properties of the x_0 space within diffusion models. Our approach integrates semantic matching, appearance transfer, and latent deviation, ensuring the maintenance of structural integrity and information fidelity during fine-grained detail transfer. A key aspect of our success is the seamless transition from x_0 space to latent space. This enables natural and accurate appearance transfers without necessitating extensive model training or fine-tuning. Comprehensive experiments across various categories and domains have thoroughly validated the versatility and robustness of our method. Our work enhances the diffusion-based models in precise and detailed image translation tasks.

As future directions, we plan to extend our focus to the broader context of general image transfer with an emphasis on fine-grained details. This expansion aims to further refine and apply our framework to a wider range of image translation scenarios, addressing more diverse and complex challenges in the field. Our future work will explore the potential of fine-grained transfer in various general image contexts, pushing the boundaries of what is achievable with current image translation technologies.

6. Supplementary Details and Extended Analysis

6.1. Detailed Derivation of the Transformation Process

We present a detailed derivation of our transformation process, focusing on the transition from the initial latent variable representation to the modified latent representation in the context of fine-grained appearance transfer. Given an initial latent variable representation x_t, it is composed of a data-informed component and a noise-driven term, formalized as:

$$x_t = \sqrt{a_t}x_0 + \sqrt{1 - a_t}\epsilon(x_t) \tag{9}$$

where x_0 represents the structured data component and $\epsilon(x_t)$ the noise term. Applying a transformation in the x_0 space, denoted by $\mathcal{T}(\cdot)$, we define a transformed latent variable x'_t as:

$$x'_t = \sqrt{a_t}(x_0 + \mathcal{T}(x'_0, x_0)) + \sqrt{1 - a_t}\epsilon(x_t) \tag{10}$$

Here, $\mathcal{T}(x'_0, x_0)$ denotes the space transformation function applied to x_0. For the optimal latent representation x^*_t, a linear combination of x_t and x'_t is considered:

$$x^*_t = \lambda x_t + (1 - \lambda)x'_t \tag{11}$$

where λ is the balancing coefficient. The noise term $\epsilon(x^*_t)$ is updated as a linear mixture:

$$\epsilon(x^*_t) = \gamma\epsilon(x_t) + (1 - \gamma)\epsilon(x'_t) \tag{12}$$

Here, γ is the mixing coefficient for the noise components. For updating from x^*_t to x^*_{t-1}, the following expression is derived:

$$x^*_{t-1} = \sqrt{\frac{a_{t-1}}{a_t}}(x^*_t - \sqrt{1 - a_t}\epsilon(x^*_t)) + \sqrt{1 - a_{t-1}}\epsilon(x^*_t) \tag{13}$$

Substituting Eqs. (10) to (12) into Eq. (13), we obtain:

$$x^*_{t-1} = \sqrt{\frac{a_{t-1}}{a_t}}(\lambda x_t + (1-\lambda)x'_t) + \kappa(\gamma\epsilon(x_t) + (1-\gamma)\epsilon(x'_t)) \tag{14}$$

where κ is defined as $\sqrt{1 - a_t} - \sqrt{\frac{a_{t-1}(1-a_t)}{a_t}}$. The final formulation of Eq. (14) can be further elaborated as:

$$\begin{aligned} x^*_{t-1} = &\sqrt{\alpha_{t-1}}(x_0 + (1 - \lambda)\mathcal{T}(x'_0, x_0)) \\ &+ \sqrt{1 - a_{t-1}}\epsilon(x^*_t) \\ &+ \sqrt{\frac{a_{t-1}(1 - a_t)}{a_t}}(\epsilon(x_t) - \epsilon(x^*_t)) \end{aligned} \tag{15}$$

In Eq. (15), the term $(1 - \lambda)\mathcal{T}(x'_0, x_0)$ indicates the shift within the x_0 space towards the target domain, while $\epsilon(x^*_t)$ guides the direction towards x^*_t. The term $\epsilon(x_t) - \epsilon(x^*_t)$ adapts to the denoising process.

6.2. Evaluation Metric

Here we employ the CLIP score [27] as a metric for evaluating semantic similarity in two distinct contexts: Text-to-Image (CLIP-T2I) and Image-to-Image (CLIP-I2I). The CLIP-T2I metric measures semantic similarity between the source prompt and the output image, whereas CLIP-I2I assesses semantic alignment between the source image and the output image. As indicated in Tab. 2, both metrics highlight the superiority of our method. We specifically emphasize the use of CLIP-T2I for capturing semantic differences, aligning with the principles of general diffusion methods [3].

Method	CLIP-T2I $\uparrow$	CLIP-I2I $\uparrow$
SplicingViT [36]	0.273	0.878
General I2I [4]	0.289	0.893
Exemplar [38]	0.268	0.872
Ours	**0.301**	**0.924**

Table 2. Comparison with Image-guided Transfer Methods on CLIP-T2I and CLIP-I2I Metric.

6.3. Generation of Detailed Descriptions for Target Images

In this section, we elucidate the process of generating detailed descriptions for target images as mentioned in Sec. 4 and illustrated in Fig. 6 of the main paper. Leveraging the multimodal input capabilities of online ChatGPT-4 [25], as demonstrated in Fig. 11, we input specific text along with target images to obtain descriptive outputs.

Our findings reveal that ChatGPT-4 demonstrates a robust capability for recognizing fine-grained categorical details and comprehending color and appearance aspects. However, it occasionally yields erroneous results in specific scenarios, such as heterochromia. To address these inaccuracies, we employed manual corrections post-hoc to ensure the precision of the textual outputs. This approach enabled us to refine the descriptions to more accurately match the visual characteristics of the target images.

6.4. Data Set Collection

In the main paper, we focus on several common animal species, including Horses, Cows, Cats, Dogs, Lions, Otters, Pandas, Foxes, and Tigers. Additionally, for generation purposes, we specified certain specific breeds within these categories to capture distinct appearance traits. For instance, in the case of dogs, we included breeds such as Corgis, Siberian Huskies, Border Collies, and Doberman Pinschers.
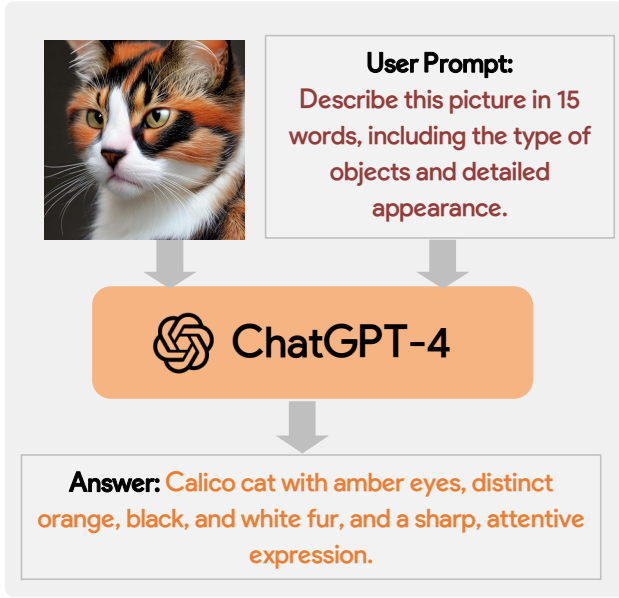
Figure 11. Illustration of generating detailed descriptions using ChatGPT-4 with multimodal input capabilities.

6.5. Comparison of DIFT Matching Strategies

In the main paper, we utilize a progressive DIFT matching strategy within the x_0 space. Alternatively, DIFT matching can be implemented from the start by directly comparing the source and target images. As shown in Fig. 12, both approaches lead to relatively stable generative outcomes, as they both facilitate the establishment of relatively accurate matching relationships. While the progressive matching method emphasizes a transition in semantic granularity from coarse to fine, the initial matching approach offers the advantage of reducing the time spent in the matching phase.

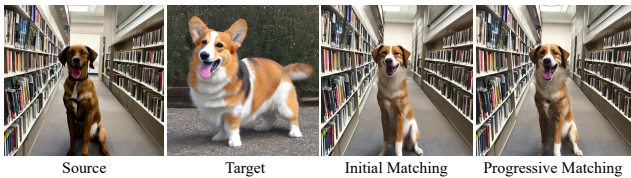| Source | Target | Initial Matching | Progressive Matching |

Figure 12. Illustration of Progressive and Initial DIFT Matching Strategies.

7. More Experimental Result

In this section, we present additional experimental results. Fig. 13 shows the face appearance transfer between animals of similar and different categories. Fig. 14 illustrates appearance transfers among different vehicles, while Fig. 15 shows fine-grained transfers focusing on specific components, such as automotive wheel rims.

10

Figure 13. Demonstration of face appearance transfer between different animals. The target images represent dogs with distinct appearances, while the source images feature various animal species.
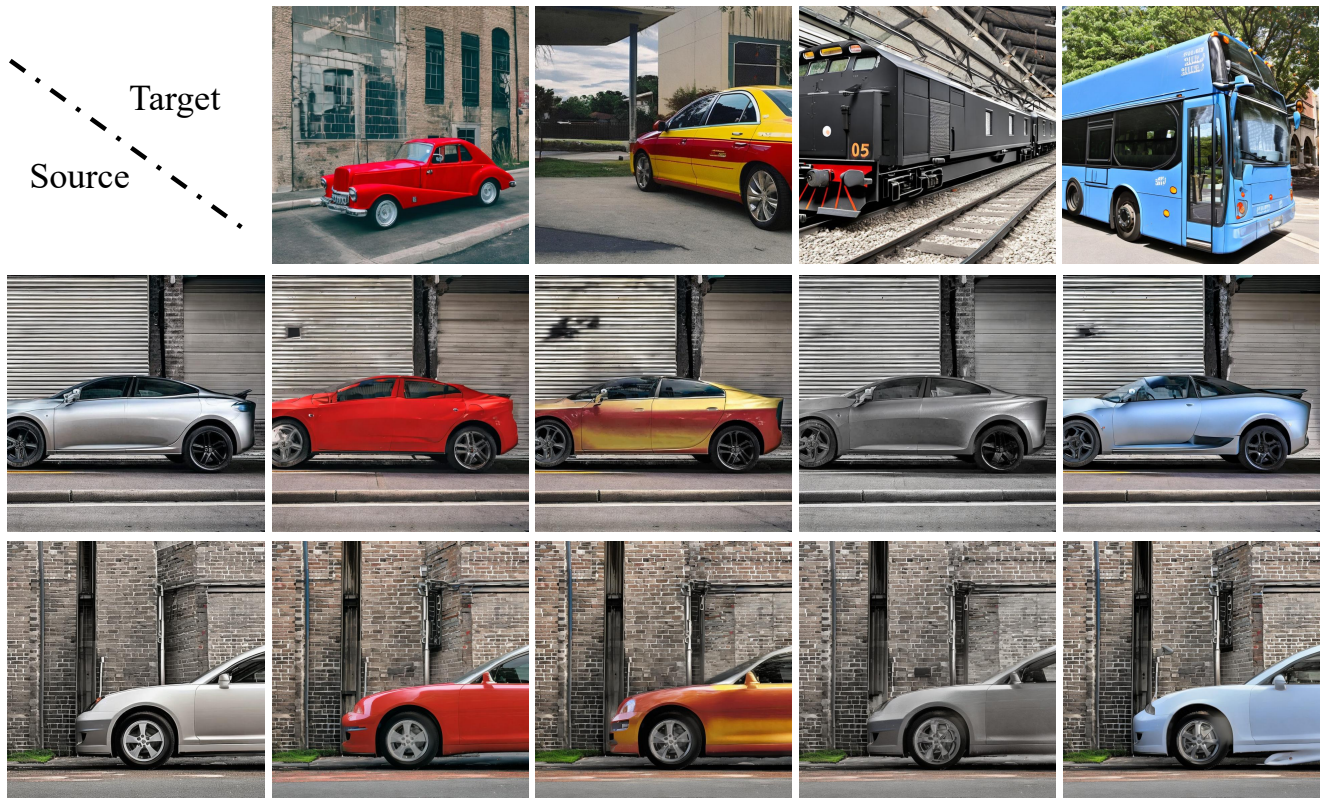
Figure 14. Appearance Transfer Results for Vehicles in Different Categories. The target images represent vehicles of various types, from left to right: a sedan, taxi, train, and bus.

Figure 15. Fine-grained appearance transfer in automotive wheels. The target images showcase, from left to right: motorcycle wheels in the first column, followed by car wheels with varying appearance from the second to the fourth column.

References

[1] Tim Brooks, Aleksander Holynski, and Alexei A Efros. Instructpix2pix: Learning to follow image editing instructions. In *Proceedings of the IEEE/CVF Conference on Computer Vision and Pattern Recognition*, pages 18392–18402, 2023. 7

[2] Mathilde Caron, Hugo Touvron, Ishan Misra, Hervé Jégou, Julien Mairal, Piotr Bojanowski, and Armand Joulin. Emerging properties in self-supervised vision transformers. In *Proceedings of the IEEE/CVF international conference on computer vision*, pages 9650–9660, 2021. 3

[3] Hila Chefer, Yuval Alaluf, Yael Vinker, Lior Wolf, and Daniel Cohen-Or. Attend-and-excite: Attention-based semantic guidance for text-to-image diffusion models. *arXiv preprint arXiv:2301.13826*, 2023. 2, 9

[4] Bin Cheng, Zuhao Liu, Yunbo Peng, and Yue Lin. General image-to-image translation with one-shot image guidance. In *Proceedings of the IEEE/CVF International Conference on Computer Vision*, pages 22736–22746, 2023. 2, 3, 6, 9

[5] Yunjey Choi, Minje Choi, Munyoung Kim, Jung-Woo Ha, Sunghun Kim, and Jaegul Choo. Stargan: Unified generative adversarial networks for multi-domain image-to-image translation. In *Proceedings of the IEEE conference on computer vision and pattern recognition*, pages 8789–8797, 2018. 2

[6] Navneet Dalal and Bill Triggs. Histograms of oriented gradients for human detection. In *2005 IEEE computer society conference on computer vision and pattern recognition (CVPR'05)*, pages 886–893. Ieee, 2005. 3

[7] Lowe David. Distinctive image features from scale-invariant keypoints. *International journal of computer vision*, 60:91–110, 2004. 3

[8] Aviv Gabbay and Yedid Hoshen. Scaling-up disentanglement for image translation. In *Proceedings of the IEEE/CVF International Conference on Computer Vision*, pages 6783–6792, 2021. 2

[9] Ian Goodfellow, Jean Pouget-Abadie, Mehdi Mirza, Bing Xu, David Warde-Farley, Sherjil Ozair, Aaron Courville, and Yoshua Bengio. Generative adversarial nets. *Advances in neural information processing systems*, 27, 2014. 2

[10] Ian Goodfellow, Jean Pouget-Abadie, Mehdi Mirza, Bing Xu, David Warde-Farley, Sherjil Ozair, Aaron Courville, and Yoshua Bengio. Generative adversarial networks. *Communications of the ACM*, 63(11):139–144, 2020. 3

[11] Amir Hertz, Ron Mokady, Jay Tenenbaum, Kfir Aberman, Yael Pritch, and Daniel Cohen-Or. Prompt-to-prompt image editing with cross attention control. *arXiv preprint arXiv:2208.01626*, 2022. 2

[12] Jonathan Ho, Ajay Jain, and Pieter Abbeel. Denoising diffusion probabilistic models. *Advances in neural information processing systems*, 33:6840–6851, 2020. 3

[13] Susung Hong, Gyuseong Lee, Wooseok Jang, and Seungryong Kim. Improving sample quality of diffusion models using self-attention guidance. In *Proceedings of the IEEE/CVF International Conference on Computer Vision*, pages 7462–7471, 2023. 3

[14] Xun Huang, Ming-Yu Liu, Serge Belongie, and Jan Kautz. Multimodal unsupervised image-to-image translation. In *Proceedings of the European conference on computer vision (ECCV)*, pages 172–189, 2018. 2

[15] Phillip Isola, Jun-Yan Zhu, Tinghui Zhou, and Alexei A Efros. Image-to-image translation with conditional adversarial networks. In *Proceedings of the IEEE conference on computer vision and pattern recognition*, pages 1125–1134, 2017. 2

[16] Bahjat Kawar, Shiran Zada, Oran Lang, Omer Tov, Huiwen Chang, Tali Dekel, Inbar Mosseri, and Michal Irani. Imagic: Text-based real image editing with diffusion models. In *Proceedings of the IEEE/CVF Conference on Computer Vision and Pattern Recognition*, pages 6007–6017, 2023. 2

[17] Gihyun Kwon and Jong Chul Ye. Diffusion-based image translation using disentangled style and content representation. *arXiv preprint arXiv:2209.15264*, 2022. 2

[18] Gihyun Kwon and Jong Chul Ye. Improving diffusion-based image translation using asymmetric gradient guidance. *arXiv preprint arXiv:2306.04396*, 2023. 2, 3

[19] Yahui Liu, Enver Sangineto, Yajing Chen, Linchao Bao, Haoxian Zhang, Nicu Sebe, Bruno Lepri, Wei Wang, and Marco De Nadai. Smoothing the disentangled latent style space for unsupervised image-to-image translation. In *Proceedings of the IEEE/CVF Conference on Computer Vision and Pattern Recognition*, pages 10785–10794, 2021. 2

[20] Naoki Matsunaga, Masato Ishii, Akio Hayakawa, Kenji Suzuki, and Takuya Narihira. Fine-grained image editing by pixel-wise guidance using diffusion models. *arXiv preprint arXiv:2212.02024*, 2022. 2

[21] Ron Mokady, Amir Hertz, Kfir Aberman, Yael Pritch, and Daniel Cohen-Or. Null-text inversion for editing real images using guided diffusion models. In *Proceedings of the IEEE/CVF Conference on Computer Vision and Pattern Recognition*, pages 6038–6047, 2023. 3, 6, 7

[22] Chong Mou, Xintao Wang, Jiechong Song, Ying Shan, and Jian Zhang. Dragondiffusion: Enabling drag-style manipulation on diffusion models. *arXiv preprint arXiv:2307.02421*, 2023. 3

[23] Chong Mou, Xintao Wang, Liangbin Xie, Jian Zhang, Zhongang Qi, Ying Shan, and Xiaohu Qie. T2i-adapter: Learning adapters to dig out more controllable ability for text-to-image diffusion models. *arXiv preprint arXiv:2302.08453*, 2023. 7

[24] Jiteng Mu, Shalini De Mello, Zhiding Yu, Nuno Vasconcelos, Xiaolong Wang, Jan Kautz, and Sifei Liu. Coordgan: Self-supervised dense correspondences emerge from gans. In *Proceedings of the IEEE/CVF Conference on Computer Vision and Pattern Recognition*, pages 10011–10020, 2022. 3

[25] OpenAI. Gpt-4 technical report. *ArXiv*, abs/2303.08774, 2023. 5, 7, 9

[26] William Peebles, Jun-Yan Zhu, Richard Zhang, Antonio Torralba, Alexei A Efros, and Eli Shechtman. Gan-supervised dense visual alignment. In *Proceedings of the IEEE/CVF Conference on Computer Vision and Pattern Recognition*, pages 13470–13481, 2022. 3

[27] Alec Radford, Jong Wook Kim, Chris Hallacy, Aditya Ramesh, Gabriel Goh, Sandhini Agarwal, Girish Sastry,

Amanda Askell, Pamela Mishkin, Jack Clark, et al. Learning transferable visual models from natural language supervision. In *International conference on machine learning*, pages 8748–8763. PMLR, 2021. 7, 9

[28] Aditya Ramesh, Prafulla Dhariwal, Alex Nichol, Casey Chu, and Mark Chen. Hierarchical text-conditional image generation with clip latents. *arXiv preprint arXiv:2204.06125*, 1 (2):3, 2022. 2

[29] Robin Rombach, Andreas Blattmann, Dominik Lorenz, Patrick Esser, and Björn Ommer. High-resolution image synthesis with latent diffusion models. In *Proceedings of the IEEE/CVF Conference on Computer Vision and Pattern Recognition*, pages 10684–10695, 2022. 2, 5, 7

[30] Chitwan Saharia, William Chan, Saurabh Saxena, Lala Li, Jay Whang, Emily L Denton, Kamyar Ghasemipour, Raphael Gontijo Lopes, Burcu Karagol Ayan, Tim Salimans, et al. Photorealistic text-to-image diffusion models with deep language understanding. *Advances in Neural Information Processing Systems*, 35:36479–36494, 2022. 2

[31] Christoph Schuhmann, Romain Beaumont, Richard Vencu, Cade Gordon, Ross Wightman, Mehdi Cherti, Theo Coombes, Aarush Katta, Clayton Mullis, Mitchell Wortsman, et al. Laion-5b: An open large-scale dataset for training next generation image-text models. *arXiv preprint arXiv:2210.08402*, 2022. 2

[32] Piyush Sharma, Nan Ding, Sebastian Goodman, and Radu Soricut. Conceptual captions: A cleaned, hypernymed, image alt-text dataset for automatic image captioning. In *Proceedings of the 56th Annual Meeting of the Association for Computational Linguistics (Volume 1: Long Papers)*, pages 2556–2565, 2018. 2

[33] Jiaming Song, Chenlin Meng, and Stefano Ermon. Denoising diffusion implicit models. *arXiv preprint arXiv:2010.02502*, 2020. 3, 4

[34] Xuan Su, Jiaming Song, Chenlin Meng, and Stefano Ermon. Dual diffusion implicit bridges for image-to-image translation. *arXiv preprint arXiv:2203.08382*, 2022. 2

[35] Luming Tang, Menglin Jia, Qianqian Wang, Cheng Perng Phoo, and Bharath Hariharan. Emergent correspondence from image diffusion. *arXiv preprint arXiv:2306.03881*, 2023. 2, 3, 4, 5

[36] Narek Tumanyan, Omer Bar-Tal, Shai Bagon, and Tali Dekel. Splicing vit features for semantic appearance transfer. In *Proceedings of the IEEE/CVF Conference on Computer Vision and Pattern Recognition*, pages 10748–10757, 2022. 2, 6, 9

[37] Po-Wei Wu, Yu-Jing Lin, Che-Han Chang, Edward Y Chang, and Shih-Wei Liao. Relgan: Multi-domain image-to-image translation via relative attributes. In *Proceedings of the IEEE/CVF international conference on computer vision*, pages 5914–5922, 2019. 2

[38] Binxin Yang, Shuyang Gu, Bo Zhang, Ting Zhang, Xuejin Chen, Xiaoyan Sun, Dong Chen, and Fang Wen. Paint by example: Exemplar-based image editing with diffusion models. In *Proceedings of the IEEE/CVF Conference on Computer Vision and Pattern Recognition*, pages 18381–18391, 2023. 2, 6, 7, 9

[39] Zili Yi, Hao Zhang, Ping Tan, and Minglun Gong. Dualgan: Unsupervised dual learning for image-to-image translation. In *Proceedings of the IEEE international conference on computer vision*, pages 2849–2857, 2017. 2

[40] Junyi Zhang, Charles Herrmann, Junhwa Hur, Luisa Polania Cabrera, Varun Jampani, Deqing Sun, and Ming-Hsuan Yang. A tale of two features: Stable diffusion complements dino for zero-shot semantic correspondence. *arXiv preprint arXiv:2305.15347*, 2023. 2, 3, 6

[41] Yuxuan Zhang, Huan Ling, Jun Gao, Kangxue Yin, Jean-Francois Lafleche, Adela Barriuso, Antonio Torralba, and Sanja Fidler. Datasetgan: Efficient labeled data factory with minimal human effort. In *Proceedings of the IEEE/CVF Conference on Computer Vision and Pattern Recognition*, pages 10145–10155, 2021. 3